

FORMULATION AND CHARACTERIZATION OF GDL-BASED ARTESUNATE SOLID LIPID NANOPARTICLE

ANAMIKA JAIN* , S. P. VYAS

Drug Delivery and Research Laboratory, Department of Pharmaceutical Sciences, Dr. Harisingh Gour University, Sagar-470003, M. P., India
*Corresponding author: Anamika Jain; *Email: jaina909@gmail.com

Received: 18 Jul 2023, Revised and Accepted: 02 Aug 2023

ABSTRACT

Objective: The present research aimed to prepare and characterize glyceryl dilaurate (GDL) containing solid lipid nanoparticles (SLN) with tween 80 and lecithin as an emulsifier in which the artesunate drug was loaded.

Methods: SLNs were synthesized by solvent emulsification-diffusion technique. The formulation was characterized for size, size distribution, zeta potential, shape and morphology, and DSC. *In vitro* drug release studies were performed at pH 5.0 and pH 7.4 to mimic *in vivo* conditions. Hemolytic studies and *In vitro*, antiplasmodial activities were carried out. *Plasmodium berghei* (NK65 resistant strain) infected mice were used to test the *in vivo* antimalarial efficacy of SLN.

Results: SLN exhibited 327 nm average sizes with 0.164 PDI and -23.4 mV zeta potential. TEM images revealed a spherical structure. The entrapment efficiency of the ART was calculated as 85.68%. *In vitro*, drug release studies showed that entrapped drug was released in a weakly acidic environment (83.45% for ART). Hemolytic studies revealed that ART-GDL conjugate was stable and safe for parenteral delivery. IC50 value of the GDL-based ART-SLNs was calculated to be 0.32 μ M. Furthermore, the GDL-based ART-SLNs resulted in enhanced parasite killing in *P. berghei*-infected mice and improved survivability as compared to free ART administration.

Conclusion: The present research allows safe and effective intravenous administration of artesunate. Thus GDL-Based ART-SLNs could be a potential drug delivery system for antimalarial therapy.

Keywords: Malaria, RBCs, Glyceryldilaurate

© 2023 The Authors. Published by Innovare Academic Sciences Pvt Ltd. This is an open access article under the CC BY license (<https://creativecommons.org/licenses/by/4.0/>)
DOI: <https://dx.doi.org/10.22159/ijap.2023v15i5.48913>. Journal homepage: <https://innovareacademics.in/journals/index.php/ijap>

INTRODUCTION

Malaria is caused by the Plasmodium parasite and is transmitted through the bites of infected female anopheles. Malaria remains a constant challenge worldwide and according to WHO 2022 report, there were approx. 247 million cases of malaria were reported in 2021 worldwide [1]. The majority of cases are reported in the South African region, South East Asia, and Eastern Mediterranean regions. Children under the age of 5 y and pregnant women are at higher risk [2]. In 1940, chloroquine shows promising results; however, the development of resistance has been observed in the case of *P. falciparum*. Thus the emergence of resistance has put pressure on public health systems to search for and develop novel antimalarial drug therapy [3]. Nanotechnology seems to be a promising strategy to overcome not only resistance as well as reduce side effects but it also improves the therapeutic index of combinatorial drugs [4].

Artesunate is a semisynthetic derivative of artemisinin obtained from the Chinese herb Artemisin annual. ART is one of the safe and highly effective antimalarial drugs [5]. World Health Organization (WHO) recommended artemisinin-based combination therapy for the treatment of multidrug-resistant against *Plasmodium Vivax* and *P. falciparum* malaria [6]. ART is a widely used drug in sub-Saharan Africa and South-East Asia for the treatment of uncomplicated malaria [7]. Apart from malaria, it is also used for the inhibition of uncontrolled division of cancer cells due to the induction of apoptosis ability in several solid tumors *in vitro* [8]. The unique 1, 2,4-trioxane structure, which contains an endoperoxide bridge is a prerequisite for its antimalarial activity. Heme present in the food vacuole of plasmodium interacts with the endoperoxide bridge of ART and activates it. The generation of reactive oxygen species subsequently binds to membrane protein and induces lipid peroxidation and, ultimately lysis of the *plasmodium* parasite [9]. Short half-life and rapid metabolism; however, limit the application of ART. Thus ART is administered in combination with a drug having a longer half-life [10].

Solid lipid nanoparticles (SLNs) are identical to o/w emulsion, except the liquid lipid is replaced by solid lipids at room

temperature. Both hydrophilic and hydrophobic drugs can be incorporated into SLNs [11]. Various advantages offered by SLNs include small size, greater surface area, enhanced bioavailability, high drug loading, protection of active pharmaceutical ingredients, and enhanced penetration of topical preparation. SLNs containing various marketed products are available in the market [12]. SLNs are usually sphere-shaped colloidal systems having a size range between 50-1000 nm [13]. Solid lipids used in the SLNs preparation include triglycerides, diacylglycerol, a mixture of mono-, di- and triglycerides, waxes, fatty acids (lauric/stearic/myristic acid), and fatty alcohols. The selection of appropriate emulsifiers, a combination of emulsifiers, and their concentration is crucial in the preparation of SLNs. Most of the emulsifiers are derived from mono or diacylglycerol or alcohol. Diacylglycerol has better emulsification and hydrophilic properties due to the free-OH group presented in its structure [14]. Nonionic emulsifiers are tween 20, 40, and 80, due to their high interfacial properties, have been widely used in the preparation of nanoemulsion [15].

Resistance against artemisinin requires an adjuvant therapy with different mechanisms to help complete the eradication of *P. falciparum*. Glyceryldilaurate is a nutritional requirement of the plasmodium parasite. Fatty acid synthesis is very important for Plasmodium species because fatty acid plays a crucial role in the synthesis of new organelles. New organelles synthesis takes place when the plasmodium is turning from the ring stage into schizont (a collection of merozoites) or the gametocyte stage. Fatty acids are also important components in the membrane synthesis of Plasmodium parasite [16].

In the current research, we have designed and developed artesunate loaded SLNs by modified solvent emulsification diffusion technique where GDL was used as a solid lipid and lecithin and tween 80 is used as an emulsifier. We hypothesize that ART-GDL SLNs have carrier, targeting, and antimalarial functionalities. ART-GDL SLNs can be selectively targeted to iRBCs due to lipids as a nutritional requirement of plasmodium parasite, thus exhibiting better antimalarial activity.

MATERIALS AND METHODS

Materials

Artesunate (ART, purity $\geq 99\%$) was obtained as a gift sample from Ipca Laboratories Limited, Ratlam (M. P.). Glyceryldilaurate (GDL) was procured as a gift sample from Subhash Chemical Industries, Pune, Maharashtra. Phospholipon® 90H (HSPC) was received as a gift sample from Lipoid GmbH Germany. Phosphatidylcholine content was approximately 97%. Tween 80 was purchased from Sigma-Aldrich Chemical Co. Distilled water was purified using a Milli-Q system. All other solvents and reagents used were of analytical grade and used without further purification.

Preparation of slns

A modified microemulsion dilution technique was used to prepare GDL-based ART-SLNs [17, 18]. Briefly, ART (100 mg) was dispersed in melted GDL (500 mg) (60-70 °C) in a water bath with continuous stirring. Separately, an aqueous emulsifier mixture containing 2.5% w/w of Tween 80 (surfactant) and 2.5% w/w of lecithin (co-surfactant) was stirred at 1200 rpm for 10 min at the same temperature. Under mild mechanical stirring, the emulsifier mixture was then added to the ART-GDL mixture. The hot microemulsion was formed by mixing two phases, then added dropwise to the ice-cold water and homogenized for 1 h at 9000 rpm. GDL-based ART-SLNs were formed and then subjected to sonication. Blank SLNs were prepared using the same procedure except for the addition of ART. Purification of GDL-based ART-SLNs was carried out to separate the excess raw material from the formulation. For that, ultracentrifugation was carried out at 35000 rpm for 1 h. at 15 °C. In the bottom of the tube, GDL-based ART-SLNs have appeared as pellets while excess raw materials are present in the supernatant. Pellet was collected from the bottom of the tube and further resuspended in purified water and sonicated for 10 min [19].

Characterization of Gdl-based Art-slns

Particle size, PDI, and zeta potential

Particle size, polydispersity index (PDI), and zeta potential (ZP) of GDL-based ART-SLNs were determined by Dynamic Light Scattering (DLS) using Zetasizer Nano ZS90 (Malvern Instruments Ltd., UK). In brief, GDL-based ART-SLNs were diluted with deionized water and then transferred to a quartz cuvette and then analyzed for size, PDI, and ZP.

Transmission electron microscopy (TEM)

Shape and surface morphology of the GDL-based ART-SLNs were characterized by Transmission Electron Microscopy (FEI, TECNAI G², S-Twin, transmission electron microscope, Netherland). For shape analysis, the formulation was placed on a carbon-coated copper grid. Excess of the solution was drained off with filter paper. The grid was air-dried and the formulation was viewed under the TEM instrument.

Differential scanning calorimetry (DSC)

DSC measures the heat gain or loss resulting from chemical or physical changes within a sample as a function of temperature. DSC scanning calorimetry analysis of drug and excipients is performed (NET ZSCH STA 449 FI, leading thermal analysis). The DSC analysis was conducted using the Perkin-Elmer model at a temperature gradient of 20 °C/min. The sample was heated at a range of 30-300 °C at a scan rate of 10 °C/min.

Entrapment efficiency

GDL-based ART-SLNs were weighed on an analytical balance for obtaining yield. Encapsulation efficiency was determined by dissolving 100 mg of GDL-based ART-SLNs in 10 ml of methanol and further sonicated for 10 min for complete solubilization of lipid. The resultant solution was transferred in a centrifuge tube and further centrifuged at 10,000 rpm for 15-20 min (Remi Instruments Pvt. Ltd., India). UV-spectroscopy of the supernatant was carried out after filtering through Whatman Anodisc 25, a filter of pore size 2µm. Absorbance was taken at 228 nm against a blank solution. Percentage encapsulation efficiency was calculated using the following equation [20].

$$\text{Entrapment Efficiency (\%)} = \frac{\text{Amount of drug in SLNs}}{\text{Total amount of drug added}} \times 100\%$$

In vitro drug release study

In vitro, drug release studies of ART from GDL-based ART-SLNs were carried out by using the dialysis bag diffusion technique described by Yang *et al.* [16] at 37 °C for 24 h at various pH values under the sink condition. Dialysis bags were placed in PBS buffer at pH 7.4 overnight before being used in the experiment. Then, 10 ml of the formulation containing 1000 µg/ml concentration equivalent to ART was placed in the cellulose membrane dialysis tube (Mw cut off: 3500). Dialysis bags were tied at both ends, and the formulation containing dialysis tubes were immersed in 200 ml of PBS buffer (pH 7.4) or PBS buffer (pH 5) and 0.5 % Tween-80 and incubated at 37 °C. The dissolution media (10 ml) was taken out at different time intervals and replaced with an equal volume of fresh buffer to maintain the sink condition. The concentration of free drug was measured for artesunate by using UV spectroscopy at λ_{max} 228 nm. All the measurements were carried out in triplicate.

Hemolysis study

Hemolytic characteristics of GDL-based ART-SLNs were investigated using rat red blood cells (RBCs). A fresh rat blood sample (2 ml) was collected in a vial. Erythrocytes suspension in sterile PBS and 20 % triton X 100 was used as a negative and positive control, respectively. Free ART and GDL-based ART-SLNs were added to the RBCs suspension, incubated for 1 h at 37±1 °C, and then centrifuged at 5000 rpm for 15 min to remove any non-hemolyzed erythrocytes and ghosts. Furthermore, the GDL-based ART-SLNs in the supernatant were removed with a Millipore Ultrafree-PF filter (Cat. No. UFP1 THK BK, Millipore). Then released Hb was measured in the supernatant by ultraviolet spectroscopy at 540 nm and percentage hemolysis was calculated [21].

$$\text{Percent hemolysis} = \frac{(A_t - A_n)}{(A_p - A_n)} \times 100\%$$

Where A_t is the absorbance of the treatment group, A_p is a positive control and A_n belongs to a negative control.

In vitro antimalarial activity

In vitro Malaria SYBR Green I-based fluorescence assay was used to explore the antimalarial activity of the GDL-based ART-SLNs and equivalent free ART. In brief, the 3D7 strain of plasmodium falciparum was maintained in human RBCs consisting of RPMI 1640 medium supplemented with 25 mmol HEPES, 1% glucose, 0.23% sodium bicarbonate, and 10% type human AB serum. The humidified atmosphere with 5% CO₂, and 5% O₂ with a desired supply of N₂ at 37 °C was maintained using a CO₂ incubator to perform the assays. Stock solutions of each of the test formulations and free ART (distilled water with 5% sodium bicarbonate), were added into an asynchronous culture of the parasite (2-3% parasitemia and 2-3% of hematocrit) in a 96-well plate. Culture medium without drug was considered as blank control and culture medium without parasitemia was used as a positive control. After an incubation period of 48 h, 50 µl of lysis buffer containing SYBR Green I staining solution was added to each well and then incubated for 30 min in darkness at room temperature. After that, fluorescence was recorded by microplate fluorometer with excitation and emission wavelength at 485 and 538 nm, respectively. IC50 value and percent parasitic inhibition were calculated using GraphPad Prism software.

Antimalarial efficacy studies in the murine malaria model

Antimalarial studies were performed after getting approval from the Institutional Animal Ethics Committee of the Department of Pharmaceutical Sciences, Dr. Harisingh Gour Vishwavidyalaya, Sagar (M. P.). All the experiments were carried out as per the guidelines of the Committee for the Purpose of Control and Supervision of Experiments on Animals (CPCSEA). Specific pathogens-free six-eight weeks old male Swiss mice (20-25 g) were selected and used for the experiment. A standard pellet diet and water *ad libitum* were provided for all the mice.

Modified Peter's 4 d suppressive test protocol

Modified Peter's 4 d suppressive test was used for the evaluation of the antimalarial efficacy of GDL-based ART-SLNs in *P. berghei*-infected murine malaria model [22]. Mice were randomly divided

into three experimental groups (n=5). *Plasmodium berghei* (NK65) resistant strain was obtained from the National Institute of Malaria Research (NIMR), New Delhi (India), and was used as a source of parasites. *P. berghei* NK65 infection was initiated by intraperitoneal (i. p.) injection of 10^6 infected RBCs except normal one. Geimsa staining thin blood smear was used for the monitoring progress of infection. Normal control animals received saline solution (0.2 ml). Free ART was dissolved in 5% NaHCO_3 in sterile distilled water and further diluted with saline. On the day '5' postinfection i. p. injection of the formulations was given for 4 consecutive days. Blood was withdrawn by the tail vein and parasitemia was observed by examining a thin blood smear under the optical microscope. 2-3 drops of blood were taken on a glass slide smeared and air dried then fixed with methanol and further stained with Geimsa dye to count parasites per thousand RBCs per slide. Negative results were considered after treatment if plasmodium was not observed in 10 microscopic fields. The mice were monitored for survival till 21 d post-infection. The % parasitemia was calculated as follows:

$$\text{Parasitemia (\%)} = \frac{\text{Number of Parasited RBCs}}{\text{Total number of RBCs examined}} \times 100\%$$

Statistical analysis

Data obtained from the drug release was evaluated using GraphPad Prism 7.0 software and expressed as the mean and standard error of the mean.

RESULTS

Particle size and polydispersity index (PDI) analysis

Particle size is one of the most significant determinants of biological fate, *in vivo* distribution, and targeting ability of the SLNs. Particle size distribution is used to determine the size range of drug-loaded SLNs, to ascertain that formulations are in the nano range. An emulsion containing non-ionic surfactant exhibited a larger size as obtained from ionic surfactant. The combination of lecithin and non-ionic

surfactant also tended to increase the size of nanoparticles. Various reports are available which demonstrated the importance of emulsifiers on the particle size of lipid nanoparticles on microemulsion-based SLN [23]. Cavalli *et al.* prepared SLNs by taking stearic acid as the lipid phase and compared the effect of ionic and non-ionic surfactants on particle size. SLNs prepared by non-ionic surfactants were of a larger size as compared to ionic surfactants. The average particle size and polydispersity index of the formulation were found to be 327 nm and 0.164, respectively as shown in fig. 1(A) Zeta potential of the GDL-based ART-SLNs was -23.4 mV (fig. 1B).

Entrapment efficiency

The entrapment efficiency of the GDL-based ART-SLNs formulation was 85.68%. The key factor to determine whether ART would be firmly incorporated or expelled into the GDL-based ART-SLNs is the lipid crystalline structure, which is related to the chemical nature of lipids. Drug expulsion is caused due to lipids that form a high crystalline state. Lattice defects in the lipid could provide more space to accommodate the active medicaments. The greater entrapment efficiency of SLNs was due to the less ordered arrangement of lipids, wherein enhanced imperfection may allow drug molecule incorporation into the lipid matrix [24].

Transmission electron microscopy (TEM)

The physical state of SLNs is of great significance from the biopharmaceutical as well as technological point of view. Morphology studies of the GDL-based ART-SLNs were carried out by using Transmission electron microscopy (TEM). TEM images of ART-loaded SLNs confirm that GDL-based ART-SLNs are spherical (fig. 2). TEM images indicated that there is no apparent change in appearance due to the entrapment of the drug. The size of the GDL-based ART-SLNs obtained by TEM was smaller than dynamic light scattering (DLS) results. The difference in size may be attributed to the shrinkage of GDL-based ART-SLNs in a dried state during the preparation of a sample of TEM [25].

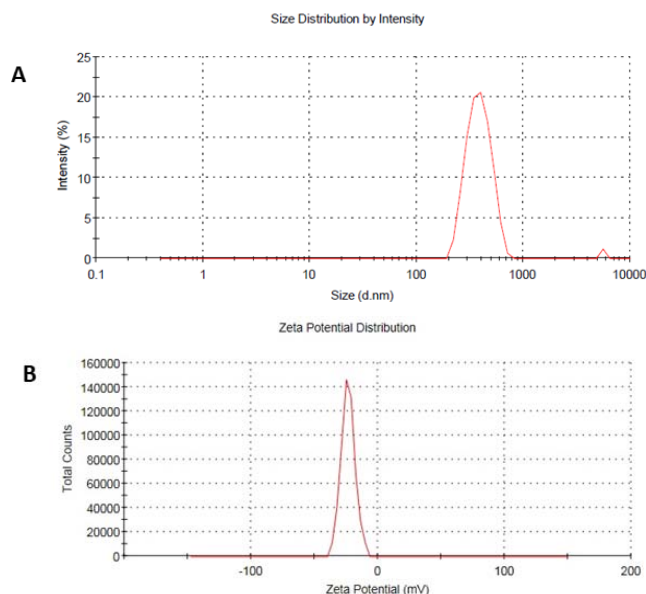


Fig. 1: (A) Particle size distribution of GDL-based ART-SLNs. (B) Zeta potential of GDL-based ART-SLNs

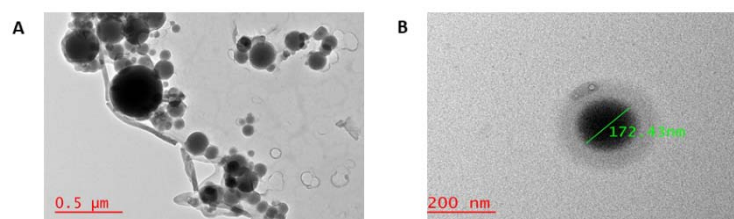


Fig. 2: (A) TEM images of GDL-based ART-SLNs (B) Enlarge TEM image

Differential scanning calorimetry (DSC) studies

DSC thermogram of pure artesunate is typical of an anhydrous crystalline drug. A sharp endothermic peak at 142.4 °C, clearly indicates the melting point of an ART. DSC thermogram of ART, GDL, and GDL-based ART-SLNs are shown in fig. 3 A, B, and C, respectively. The disappearance of the melting peak of ART peak at 142.4 °C was found in

DSC thermograms of GDL-based ART-SLNs as compared to the thermograms of raw material. It can be inferred from the thermogram that the disappearance of the melting peak of ART may be attributed to the amorphous or molecularly dispersed structure of ART in the GDL lipid matrix. Other studies also reported the same result (absence of drug melting point) [26]. Cavalli *et al.* also reported that progesterone and hydrocortisone were present in noncrystalline form in SLNs [27].

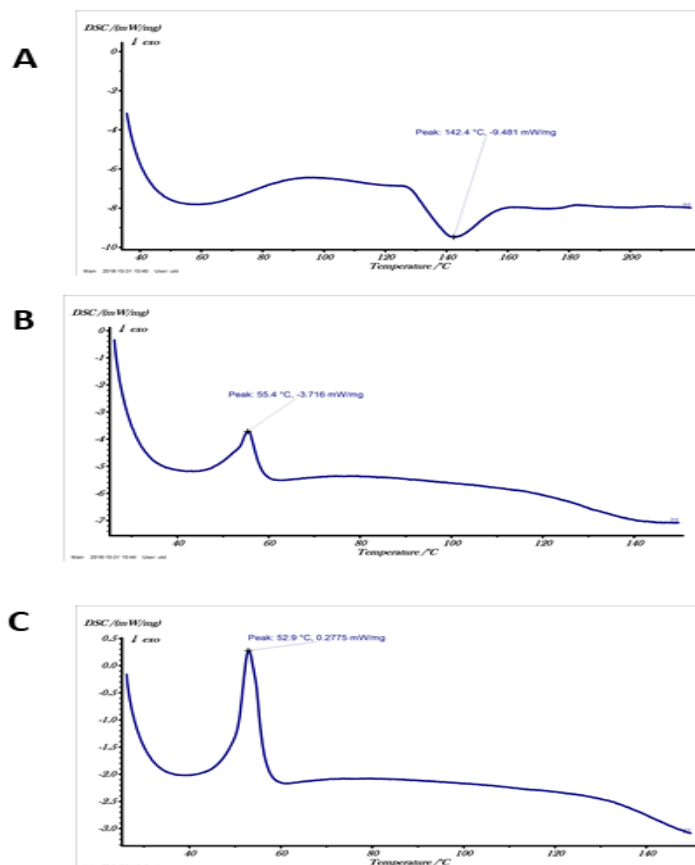


Fig. 3: DSC thermogram of (A). ART (B). GDL (C). GDL-based ART-SLNs formulation

In vitro drug release studies

In vitro, drug release profile of ART from the SLNs is shown in fig. 4. As shown in fig. 4 ART as a free drug exhibited a fast diffusion, while nanoencapsulation showed controlled drug release. The burst release is due to the adsorption of a drug on the surface of the nanoparticle and due to the peripheral migration of the drug during the maturation process of nanoparticles. In the present formulation, ART was well harbored within the lipid matrix of SLNs, hence due to the exceeding hydrophobic nature of GDL-based ART SLNs and the exclusion of surface adsorption due to the use of emulsifier(s) in optimum concentration, this resulted in slow and constant release,

without the occurrence of initial burst release. The slower release was observed from SLNs suggesting that drug release was affected due to sink condition under a concentration gradient. ART affinity for Solid lipidic phase [28]. *In vitro* drug release studies were carried out at pH 7.4 and pH 5 to mimic the *in vivo* physiological condition of blood and food vacuole of the plasmodium parasite, respectively. ART release profiles from SLNs are shown in fig. 4 at pH 7.4, ART release from SLNs was relatively slow (20.56%). Slow release at blood pH is indicative of the promising carrying ability of ART-GDL by SLNs. Additionally, at pH 5.0; GDL-based ART-SLNs showed a relatively faster release rate as approximately 83.45% of parent ART was released in 24 h.

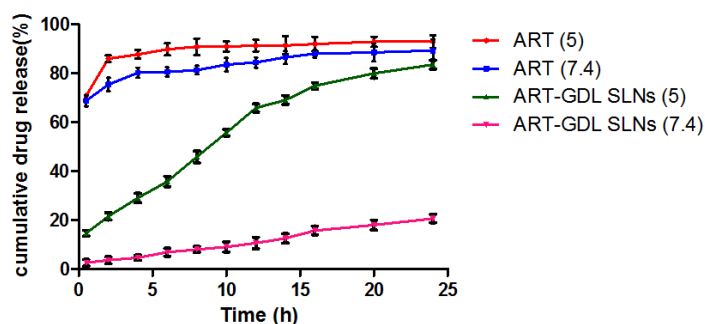


Fig. 4: Cumulative drug release of ART from GDL-based ART-SLNs at different pH (pH 7.4 and pH 5). Data are expressed as mean±SD (n=3)

Hemolysis study

Triton X-100 a known hemolytic agent, was used as a positive control in this study that caused 100% hemolysis and thus could validate the experiment. Glyceryldilaurate, lecithin, and ART showed some degree of hydrolysis as reported in earlier reports as well [29, 30]. It is supposed that the combination of all the above-mentioned components additively contributes to comparatively greater hemolysis. However, such a hemolysis pattern was not recorded in this study (fig. 5). It can be concluded that the use of the above-mentioned components in SLNs altered their mode and degree of interaction with RBCs. Thus additive effect as reported in the literature got excluded may be due to the combination of the above all components. Similar findings have also been reported for lipid emulsion by Jumma *et al.* [32] and M. Joshi *et al.* [31] It should be noted that *in vitro* hemolysis studies only provide an idea about the hemolytic character of individual components as well as in formulation. It does not correlate with *in vivo* conditions.

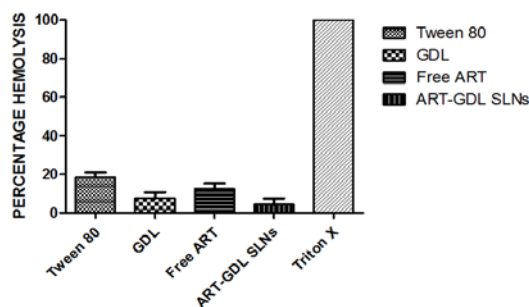


Fig. 5: Percentage hemolysis caused by excipients, free ART, and GDL-based ART-SLNs (n=3)

In vitro antimalarial activity

In vitro, antimalarial activity results showed that GDL-based ART-SLNs are active against *P. falciparum* 3D7 strain at very low concentrations. *In vitro*, the antimalarial activity of GDL-based ART-SLNs on the *P. falciparum* 3D7 strain was carried out by employing MSF protocol [33]. For mimicking *in vivo* conditions, the 3D7 RBCs culture was incubated with free ART (as control) and GDL-based ART-SLNs for 48 h. Moreover, the IC₅₀ value of the free ART and GDL-based ART-SLNs was calculated and found to be 0.80 μ M and 0.32 μ M respectively as shown in fig. 6. It indicates that SLNs have higher inhibitory effects as compared to equivalent doses of ART.

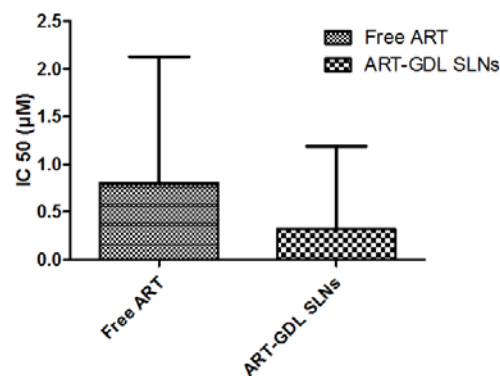


Fig. 6: *In vitro* antimalarial activity of Free ART and GDL-based ART-SLNs versus *P. falciparum* (3D7 strain). Data are presented as mean \pm SD (n=3)

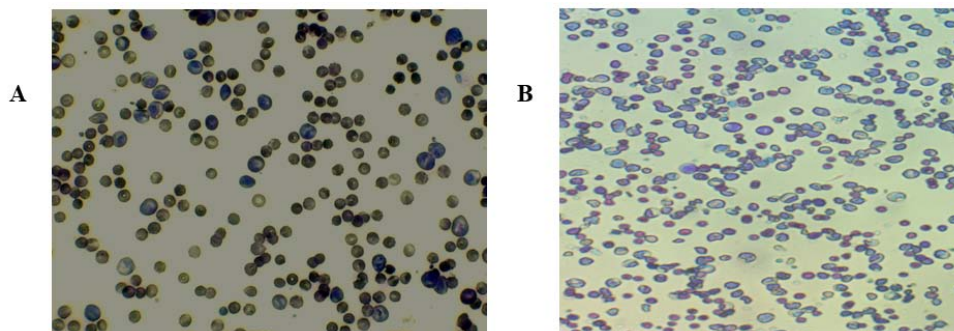


Fig. 7: Photomicrograph of the blood smears of (A) control group (B) GDL-based ART-SLNs treatment group on the 8th day at 40 x magnifications under oil immersion

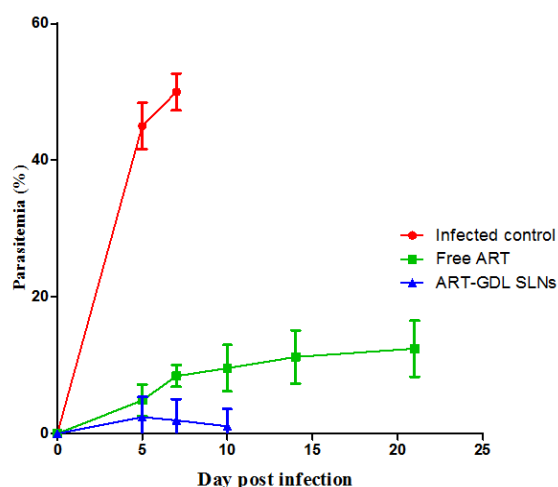


Fig. 8: *In vivo* antimalarial activity of GDL-based ART-SLNs in *P. berghei*-infected mice (n=5) as compared to ART

In vivo antimalarial efficacy

The infected mice were treated with ART and GDL-based ART-SLNs for four days. Blood smears and staining of plasmodium parasites from control and treatment groups are illustrated in fig. 7. The results of the effect of GDL-based ART-SLNs on parasitemia progression of *P. berghei*-infected mice are shown in fig. 8. On day 7, the control group showed 50 % parasitemia and followed by the death of the entire group died within a week. On day 10, the treatment group with the current formulation exhibited 1.10 % parasitemia. Thus, GDL-based ART-SLNs were effective in the complete elimination of the parasite by day 21. Additionally, GDL-based ART-SLNs enhanced the life expectancy of mice while delayed recrudescence as compared to free ART under identical conditions. The obtained results indicated that the present formulation significantly protected mice against *P. berghei* infection.

DISCUSSION

The development of GDL-based ART-SLNs has shown great potential for improving the therapeutic efficacy of poorly water-soluble drugs (artesunate). World Health Organization (WHO) recommended Artemisinin-based combination therapy for complicated malaria.

The optimum effectiveness of artemisinins is hindered by hydrophobicity, short half-life, and instability. GDL-based ART-SLNs were prepared by using a modified microemulsion dilution technique. GDL was used for SLNs preparation; particle size and size distribution are two important characteristics of SLNs, which affect drug release and biodistribution. The judicious and optimal use of emulsifier/co-emulsifier could yield SLNs of the average hydrodynamic size of 327 nm with PDI 0.164, revealing the homogeneity of SLNs regarding size and distribution. This was smaller as compared to similar studies performed by Wadzanayi *et al.*, who obtained 1109 nm particle size and 0.082 PDI [34]. Zeta potential (ZP) measures the surface charge of nanoparticles. Storage stability of the aqueous colloidal dispersion was provided by ZP. High zeta potential is required for the stability of colloidal dispersion. ZP obtained in this study is -23.4 mV. The negative charge on SLNs is due to lipid and nonionic surfactants [35]. The entrapment efficiency (EE) of the present formulation was 85.68%. The key factor to determine whether ART would be firmly incorporated or expelled into the GDL-based ART-SLNs is the lipid crystalline structure, which is related to the chemical nature of lipids. Drug expulsion is caused due to lipids that form a high crystalline state. Lattice defects in the lipid could provide more space to accommodate the active medicaments. The high EE of ART could be attributed to the increased imperfections and less ordered arrangement of the GDL matrix [24]. Further, TEM is used for the characterization of SLNs. The formulation was found devoid of aggregates which could be attributed to the emulsifier layer around individual particles, which may offer a protective barrier where the particle approach closer to each other or repelled due to surface-associated charge (zeta potential). These results are in close agreement with Paliperidone-loaded SLNs reported by Kumar *et al.* [36]. No peak of ART at 142.4 °C was detected in DSC studies of the present formulation as compared to DSC of raw materials. Loss of ART melting peak could be due to the molecularly dispersed structure or amorphous nature of ART in a lipid matrix. Previous studies also reported the absence of a melting peak of the drug in formulation [37, 38]. Drug release from SLNs is dependent on the solubility of the drug in the lipid, lipid matrix, and concentration of surfactant [39]. In this study drug release studies were carried out at two different physiological pH (blood pH 7.4 and parasitic food vacuole pH 5.0). The present formulation follows a biphasic release pattern in the first-hour initial burst release was obtained, followed by sustained release of the drug over 24 hr (fig. 4). Different release profiles from solid lipid nanoparticles (SLNs) are reported in the literature. In the present formulation, results obtained are in close agreement with the data obtained by Kelidari *et al.* [40]. They reported the initial burst release due to the large surface area of SLNs as well as the surface enrichment of the drug. Further, it was noticed that the prepared formulation was appreciatively stable in terms of drug release from SLNs was recorded to be consistent and slow provided 83.45% percentage release time over 24 h. The slow drug behavior leads to the condition of longer exposure of parasites to the drugs, which may avert the possibility of drug resistance. The hemolytic activity demonstrated that ART in SLNs is relatively safer as minimum hemolysis was recorded on an equivalent dose basis comparison with plain drug; thus, it is safe for intravenous administration. IC50 recorded in the case of the present formulation was comparatively less than the plain drug, this is attributed to the improved antiparasitic activity. This may be ascribed to the avidity of the iRBCs to mono/diglyceride, where GDL was used as a matrix of SLNs in the carrier of the drug. Further, the better activity recorded could be accounted to the accumulation of SLNs in the digestive vacuole. Similar results were also reported by Ibrahim *et al.* [37]. *In vivo*, studies demonstrated fast clearance of *P. berghei* from infected mice corroborated and substantiate improved therapeutic index of the drug when administered entrapped within the SLNs.

CONCLUSION

The results of the present study suggest that microemulsion dilution and solvent/cosolvent technique can successfully be used for the preparation of nanometric GDL-based SLNs loaded with ART. The formulation is uniform in shape, smaller in size, narrow in size distribution, and safe for intravenous administration. *In vitro* and *in*

vivo results show that the formulation has a higher antimalarial activity at a low dosage of ART. In conclusion, the GDL-based SLNs may emerge as a potential option for antimalarial therapy, which could avert the drug resistance or may be used for the purpose when given in an antimalarial combination. However, further systematic studies to explore and appreciate entail the clinical application of nanometric SLNs-based formulation.

ABBREVIATIONS

ART-Artesunate, GDL-Glyceryl dilaurate, SLNs-Solid Lipid Nanoparticles, DAG-Diacylglycerol, PBS-Phosphate Buffer Saline, RBCs-Red Blood Cells

ACKNOWLEDGEMENT

The authors are thankful to the Indian Council of Medical Research (ICMR), New Delhi, India (Grant no. 45/38/2018-PHA/BMS, Dated 24/07/2018) for providing financial assistance. The authors also show their gratitude to the Department of Pharmaceutical Sciences, Dr. Harisingh Gour University, Sagar for providing technical assistance, infrastructure, and sophisticated instrument facilities. I would like to acknowledge Mandeep Singh, Tanweer Haider and Laxmikant Goutam for their continuous support during my project work.

AUTHORS CONTRIBUTIONS

All the authors have contributed equally.

CONFLICTS OF INTERESTS

The authors declare that there are no conflicts of interest.

REFERENCES

1. World malaria report 2022: WHO; 2022.
2. Musoke D, Atusingwize E, Namata C, Ndejjo R, Wanyenze RK, Kanya MR. Integrated malaria prevention in low- and middle-income countries: a systematic review. *Malar J*. 2023;22(1):79. doi: 10.1186/s12936-023-04500-x, PMID 36879237.
3. Patel CA, Pande S, Shukla P, Ranch K, Al-Tabakha MM, Boddu SH. Antimalarial drug resistance: trends, mechanisms, and strategies to combat antimalarial resistance. *Malarial drug delivery systems: advances in treatment of infectious diseases*. Springer; 2023. p. 43-69. doi: 10.1007/978-3-031-15848-3_3.
4. Ramteke S, Ubnare R, Dubey N, Singh A. Intranasal delivery of artemether for the treatment of cerebral malaria. *Int J Pharm Pharm Sci*. 2018;10(9):9. doi: 10.22159/ijpps.2018v10i9.25408.
5. Anamika J, Nikhar V, Laxmikant G, Priya S, Sonal V, Vyas SP. Nanobiotechnological modules as molecular target tracker for the treatment and prevention of malaria: options and opportunity. *Drug Deliv Transl Res*. 2020;10(4):1095-110. doi: 10.1007/s13346-020-00770-z, PMID 32378173.
6. Bonsergent M, Tching Sin M, Honore S, Bertault Peres P, Lepelletier A, Flet L. Use of artesunate in the treatment of severe imported malaria in France: review of the effectiveness and real-life safety in two French university hospitals. *BMC Infect Dis*. 2023;23(1):359. doi: 10.1186/s12879-023-08260-6, PMID 37231336.
7. Goodman C, Tougher S, Shang TJ, Visser T. Improving malaria case management with artemisinin-based combination therapies and malaria rapid diagnostic tests in private medicine retail outlets in sub-Saharan Africa: a systematic review; 2023. doi: 10.1101/2023.05.23.23290407.
8. Marwa KJ, Kapesa A, Kamugisha E, Swedberg G. The influence of cytochrome P450 polymorphisms on pharmacokinetic profiles and treatment outcomes among malaria patients in Sub-Saharan Africa: a systematic review. *Pharmgenomics Pers Med*. 2023;16:449-61. doi: 10.2147/PGPM.S379945, PMID 3723718.
9. Niederreiter M, Klein J, Arndt K, Werner J, Mayer B. Anti-cancer effects of artesunate in human 3D tumor models of different complexity. *Int J Mol Sci*. 2023;24(9):7844. doi: 10.3390/ijms24097844, PMID 37175551.
10. Adebayo AH, Okenze GN, Yakubu OF, Abikoye ME. Biochemical and histopathological effects of coadministration of

- amodiaquine, artesunate, and selenium on plasmodium berghei infected mice. *Asian J Pharm Clin Res.* 2018;11(15):1-4. doi: 10.22159/ajpcr.2018.v11s3.29963.
11. Shukla M, Rath K, Hassam M, Yadav DK, Karnatak M, Rawat V. An overview on the antimalarial activity of 1,2,4-trioxanes, 1,2,4-trioxolanes and 1,2,4,5-tetraoxanes. *Med Res Rev.* 2023;1(2):2-4. doi: 10.1002/med.21979, PMID 37222435.
 12. Li Y, Xu E, Rong R, Zhang S, Yuan WE, Qiu M. Glutaraldehyde modified red blood cells delivering artesunate to the liver as a dual therapeutic and prophylactic antimalaria strategy. *J Mater Chem B.* 2023. doi: 10.1039/D3TB00315A, PMID 37458002.
 13. Khairnar SV, Pagare P, Thakre A, Nambiar AR, Junnuthula V, Abraham MC. Review on the scale-up methods for the preparation of solid lipid nanoparticles. *Pharmaceutics.* 2022;14(9):1886. doi: 10.3390/pharmaceutics14091886, PMID 36145632.
 14. Priyanka P, Sri Rekha M, Devi AS. Review on formulation and evaluation of solid lipid nanoparticles for vaginal application. *Int J Pharm Pharm Sci.* 2022;14(1):1-8. doi: 10.22159/ijpps.2022v14i1.42595.
 15. Alkawash S. Solid lipid nanoparticles, an effective carrier for classical antifungal drugs. *Saudi Pharm J.* 2023;31(7):1167-80. doi: 10.1016/j.jpsps.2023.05.011, PMID 37273269.
 16. Gugleva V, Andonova V. Recent progress of solid lipid nanoparticles and nanostructured lipid carriers as ocular drug delivery platforms. *Pharmaceutics (Basel).* 2023;16(3):474. doi: 10.3390/ph16030474, PMID 36986574.
 17. Xu Y, Lv Y, Zhao H, He X, Li X, Yi S. Diacylglycerol pre-emulsion prepared through ultrasound improves the gel properties of golden thread surimi. *Ultrason Sonochem.* 2022;82:105915. doi: 10.1016/j.ultrsonch.2022.105915. PMID 35042162.
 18. Tang CH, Chen HL, Dong JR. Solid lipid nanoparticles (SLNs) and nanostructured lipid carriers (NLCs) as food-grade nanovehicles for hydrophobic nutraceuticals or bioactives. *Appl Sci.* 2023;13(3):1726. doi: 10.3390/app13031726.
 19. Kamarullah W, Indrajaya E, Emmanuella J. Potency of luteolin with solid lipid nanoparticle (SLN)-polyethylene glycol (PEG) modification for artemisinin-resistant plasmodium falciparum infection. *Indonesian J Trop Infect Dis.* 2018;7(3):80. doi: 10.20473/ijtid.v7i3.6726.
 20. Boonme P, Souto EB, Wuttisantikul N, Jongjit T, Pichayakorn W. Influence of lipids on the properties of solid lipid nanoparticles from microemulsion technique. *Eur J Lipid Sci Technol.* 2013;115(7):820-4. doi: 10.1002/ejlt.201200240.
 21. Gardouh A. Design and characterization of glyceryl monostearate solid lipid nanoparticles prepared by high shear homogenization. *Br J Pharm Res.* 2013;3(3):326-46. doi: 10.9734/BJPR/2014/2770.
 22. Kumar R, Singh A, Sharma K, Dhasmana D, Garg N, Siril PF. Preparation, characterization and *in vitro* cytotoxicity of fenofibrate and nabumetone-loaded solid lipid nanoparticles. *Mater Sci Eng C Mater Biol Appl.* 2020;106:110184. doi: 10.1016/j.msec.2019.110184, PMID 31753394.
 23. Shi C, Zhang Z, Shi J, Wang F, Luan Y. Co-delivery of docetaxel and chloroquine via PEO-PPO-PCL/TPGS micelles for overcoming multidrug resistance. *Int J Pharm.* 2015;495(2):932-9. doi: 10.1016/j.ijpharm.2015.10.009. PMID 26456262.
 24. Chadha R, Gupta S, Pathak N. Artesunate-loaded chitosan/lecithin nanoparticles: preparation, characterization, and *in vivo* studies. *Drug Dev Ind Pharm.* 2012;38(12):1538-46. doi: 10.3109/03639045.2012.658812, PMID 22348223.
 25. Cavalli R, Caputo O, Marengo E, Pattarino F, Gasco MR. The effect of the components of microemulsions on both size and crystalline structure of solid lipid nanoparticles (SLN) containing a series of model molecules. *Pharmazie.* 1998;53(6):392-6.
 26. Kheradmandnia S, Vasheghani Farahani E, Nosrati M, Atyabi F. Preparation and characterization of ketoprofen-loaded solid lipid nanoparticles made from beeswax and carnauba wax. *Nanomedicine.* 2010;6(6):753-9. doi: 10.1016/j.nano.2010.06.003. PMID 20599527.
 27. Manjili HK, Malvandi H, Mousavi MS, Attari E, Danafar H. *In vitro* and *in vivo* delivery of artemisinin loaded PCL-PEG-PCL micelles and its pharmacokinetic study. *Artif Cells Nanomed Biotechnol.* 2018;46(5):926-36. doi: 10.1080/21691401.2017.1347880, PMID 28683649.
 28. Cavalli R, Peira E, Caputo O, Gasco MR. Solid lipid nanoparticles as carriers of hydrocortisone and progesterone complexes with β -cyclodextrins. *Int J Pharm.* 1999;182(1):59-69. doi: 10.1016/s0378-5173(99)00066-6, PMID 10332075.
 29. Carbone C, Fuochi V, Zielinska A, Musumeci T, Souto EB, Bonaccorso A. Dual-drugs delivery in solid lipid nanoparticles for the treatment of candida albicans mycosis. *Colloids Surf B Biointerfaces.* 2020;186:110705. doi: 10.1016/j.colsurfb.2019.110705. PMID 31830707.
 30. Nagasaka Y, Ishii F. Interaction between erythrocytes from three different animals and emulsions prepared with various lecithins and oils. *Colloids Surf B Biointerfaces.* 2001;22(2):141-7. doi: 10.1016/s0927-7765(01)00148-5, PMID 11451660.
 31. Joshi M, Pathak S, Sharma S, Patravale V. Design and *in vivo* pharmacodynamic evaluation of nanostructured lipid carriers for parenteral delivery of artemether: Nanoject. *Int J Pharm.* 2008;364(1):119-26. doi: 10.1016/j.ijpharm.2008.07.032, PMID 18765274.
 32. Jumaa M, Kleinebudde P, Muller BW. Physicochemical properties and hemolytic effect of different lipid emulsion formulations using a mixture of emulsifiers. *Pharm Acta Helv.* 1999;73(6):293-301. doi: 10.1016/S0031-6865(99)00003-5.
 33. Ismail M, Du Y, Ling L, Li X. Artesunate-heparin conjugate based nanocapsules with improved pharmacokinetics to combat malaria. *Int J Pharm.* 2019;562:162-71. doi: 10.1016/j.ijpharm.2019.03.031. PMID 30902709.
 34. Masiwa WL, Gadaga LL. Intestinal permeability of artesunate-loaded solid lipid nanoparticles using the everted gut method. *J Drug Deliv.* 2018;2018:3021738. doi: 10.1155/2018/3021738, PMID 29854465.
 35. Schubert MA, Muller Goymann CC. Characterisation of surface-modified solid lipid nanoparticles (SLN): influence of lecithin and nonionic emulsifier. *Eur J Pharm Biopharm.* 2005;61(1-2):77-86. doi: 10.1016/j.ejpb.2005.03.006. PMID 16011893.
 36. Kumar S, Randhawa JK. Preparation and characterization of paliperidone-loaded solid lipid nanoparticles. *Colloids Surf B Biointerfaces.* 2013;102:562-8. doi: 10.1016/j.colsurfb.2012.08.052, PMID 23104026.
 37. Ibrahim N, Ibrahim H, Sabater AM, Mazier D, Valentin A, Nepveu F. Artemisinin nanoformulation suitable for intravenous injection: preparation, characterization and antimalarial activities. *Int J Pharm.* 2015;495(2):671-9. doi: 10.1016/j.ijpharm.2015.09.020, PMID 26383839.
 38. Manjili HK, Malvandi H, Mousavi MS, Attari E, Danafar H. *In vitro* and *in vivo* delivery of artemisinin loaded PCL-PEG-PCL micelles and its pharmacokinetic study. *Artif Cells Nanomed Biotechnol.* 2018;46(5):926-36. doi: 10.1080/21691401.2017.1347880, PMID 28683649.
 39. Kumar S, Randhawa JK. High melting lipid-based approach for drug delivery: solid lipid nanoparticles. *Mater Sci Eng C Mater Biol Appl.* 2013;33(4):1842-52. doi: 10.1016/j.msec.2013.01.037, PMID 23498204.
 40. Kelidari HR, Saeedi M, Akbari J, Morteza Semnani K, Gill P, Valizadeh H. Formulation optimization and *in vitro* skin penetration of spironolactone loaded solid lipid nanoparticles. *Colloids Surf B Biointerfaces.* 2015;128:473-9. doi: 10.1016/j.colsurfb.2015.02.046, PMID 25797482.